

Interpretation of LHC excesses in ditop and ditau channels as a 400-GeV pseudoscalar resonance

ERNESTO ARGANDA^{1,2*}, LEANDRO DA ROLD^{3†}, DANIEL A. DÍAZ^{2‡} AND ANIBAL D. MEDINA^{2§}

¹*Instituto de Física Teórica UAM/CSIC,
C/ Nicolás Cabrera 13-15, Campus de Cantoblanco, 28049, Madrid, Spain*

²*IFLP, CONICET - Dpto. de Física, Universidad Nacional de La Plata,
C.C. 67, 1900 La Plata, Argentina*

³*Centro Atómico Bariloche, Instituto Balseiro and CONICET,
Av. Bustillo 9500, 8400, S. C. de Bariloche, Argentina*

Abstract

Since the discovery in 2012 of the Higgs boson at the LHC, as the last missing piece of the Standard Model of particle physics, any hint of new physics has been intensively searched for, with no confirmation to date. There are however slight deviations from the SM that are worth investigating. The CMS collaboration has reported, in a search for heavy resonances decaying to $t\bar{t}$ with a 13-TeV center-of-mass energy and a luminosity of 35.9 fb^{-1} , deviations from the SM predictions at the 3.5σ level locally (1.9σ after the look-elsewhere effect). In addition, in the ditau final state search performed by the ATLAS collaboration at $\sqrt{s} = 13 \text{ TeV}$ and $\mathcal{L} = 139 \text{ fb}^{-1}$, deviations from the SM at the 2σ level have been also observed. Interestingly, both slight excesses are compatible with a new pseudoscalar boson with a mass around 400 GeV that couples at least to fermions of the third generation and gluons. Starting from a purely phenomenological perspective, we inspect the possibility that a 400-GeV pseudoscalar can account for these deviations and at the same time satisfy the constraints on the rest of the channels that it gives contributions to and that are analyzed by the ATLAS and CMS experiments. After obtaining the range of effective couplings compatible with all experimental measurements, we study the gauge invariant UV completions that can give rise to this type of pseudoscalar resonance, which can be accommodated in an $SO(6)/SO(5)$ model with consistency at the 1σ level and in a $SO(5) \times U(1)_P \times U(1)_X / SO(4) \times U(1)_X$ at the 2σ level, while exceedingly large quartic couplings would be necessary to account for it in a general two Higgs doublet model.

*ernesto.arganda@csic.es

†daroldl@cab.cnea.gov.ar

‡daniel.diaz@fisica.unlp.edu.ar

§anibal.medina@fisica.unlp.edu.ar

1 Introduction

There are many searches for new physics being done at the Large Hadron Collider (LHC) but for the moment only a scalar particle that resembles the last missing piece of the Standard Model (SM) has been discovered, the Higgs [1,2]. The fact that no clear indication of signs of new physics emerges from these collider searches implies that, as phenomenologists, we should pay attention to the small but coordinated deviations from the SM behavior that may arise in different search channels as possible hints of a specific type of new physics. Interestingly, there are two particular somewhat recent searches in which this behavior seems to be happening. On one hand, in the ditop search performed by the CMS collaboration [3] at a center of mass energy $\sqrt{s} = 13$ TeV and a luminosity of $\mathcal{L} = 35.9 \text{ fb}^{-1}$, with top quarks decaying into single and dilepton final states, deviations from the SM behavior arise at the 3.5σ level locally (1.9σ after the look-elsewhere effect) that can be accounted for by a pseudoscalar with a mass around 400 GeV that couples at least to top quarks and gluons. On the other hand, in the ditau search done by the ATLAS collaboration [4] at $\sqrt{s} = 13$ TeV and $\mathcal{L} = 139 \text{ fb}^{-1}$, deviations from the SM at the 2σ level are observed which, interestingly enough, can be accounted for by pseudoscalar coupling to tau leptons, bottom-quarks and gluons, once again with a mass around 400 GeV. Furthermore, whatever new physics may account simultaneously for these possible hints should also be consistent with other collider searches to which it could provide contributions to [5–14].

In this work we consider initially from a pure phenomenological bottom-up approach the possibility that a pseudoscalar with a mass of 400 GeV is indeed responsible simultaneously for these observed hints and at the same time satisfies the constraints coming from other final states that it could contribute to and that are search for at the LHC. An idea in this direction was considered also in [15]. Considering the interactions of the pseudoscalar up to dimension-5 operators, we find that there exists a well-defined region of couplings in which the hints as well as the constraints can be satisfied at the same time. We then study the implications on the new physics of possible gauge invariant models in which a pseudoscalar with that particular mass and couplings can be obtained. We find that, given the parameter space consistent with the measurements, it turns out to be highly unlikely that the pseudoscalar could be accommodated in a two Higgs doublet model (2HDM) even in more general possible versions of it [16]. However, we show that if the pseudoscalar is associated with a pseudo-Nambu-Goldstone (pNGB) boson of broken global symmetry in composite Higgs models [17–23], one can accommodate its mass and couplings for an $SO(6)/SO(5)$ model [24, 25] with consistency and the 1σ level with the measurements, and in a $SO(5) \times U(1)_P \times U(1)_X/SO(4) \times U(1)_X$ [25] at the 2σ level.

The remainder of the work is organized as follows: in Section 2 we summarize the main experimental searches, carried out by ATLAS and CMS, for heavy resonances that give rise to small deviations from the SM expectations or that could restrict the possible parameter space. Section 3 is devoted, from a general approach of effective field theories, to the phenomenology of a 400-GeV pseudoscalar boson that can account for these experimental signatures. In Section 4 we analyze numerically the range of couplings allowed and excluded by the experimental data, while Section 5 is dedicated to the UV completions that could give rise to this 400-GeV pseudoscalar boson with the allowed couplings. Finally, we present our main conclusions in Section 6.

2 Experimental hints and constraints

In the present work we consider several searches carried out at the LHC by the ATLAS and CMS collaborations that either show a hint or lead to a constraint for a pseudoscalar, and that allow us to determine the effective couplings of the proposed new state. A brief summary of the searches

and the parameters used is presented in this section.

2.1 Final state $t\bar{t}$

A moderate excess in top quark pair production has been found by the CMS collaboration [3]. This excess has been proven to be compatible with an intermediate state consisting on a scalar or pseudoscalar boson with a mass of 400 GeV, created via gluon fusion and decaying into a top-antitop quark pair. In Ref. [3] the CMS collaboration presented a search for heavy Higgs bosons decaying into a top quark pair, in single and dilepton final states, within a data set corresponding to an integrated luminosity of 35.9 fb^{-1} and a center-of-mass energy of 13 TeV. The masses of the hypothetical scalar and pseudoscalar bosons were probed within the range 400 GeV to 750 GeV and a total relative width from 0.5 to 25% of its mass. The largest deviation from the SM background was observed for a pseudoscalar boson with a mass of 400 GeV and a total relative width of 4%, with a local significance of 3.5 ± 0.3 standard deviations. The significance of the excess became 1.9 standard deviations after accounting for the look-elsewhere effect in the mass, total width and CP-state of the new resonance. The analysis considered tree level interactions with the top quark only, as well as interactions with gluons induced at one-loop level. Under those assumptions it was found that, for $m_A = 400 \text{ GeV}$ and $\Gamma_A/m_A = 0.04$, a top coupling $g_{At\bar{t}} \approx 0.9$ yields the maximum likelihood ratio between the hypothesis of the existence of the pseudoscalar boson and the SM scenario, as can be seen in Fig. 7 of that work.¹ For $0.6 \lesssim g_{At\bar{t}} \lesssim 1$ the model exceeds the range of compatibility with the SM in more than two standard deviations, is consistent with the measurement at one standard deviation and is below a critical value which would yield a nonphysical scenario, in which the partial decay width of the pseudoscalar boson into a top-antitop pair would exceed the total decay width from that channel. In the present work we consider cross sections of the $t\bar{t}$ channel in agreement with those values of $g_{At\bar{t}}$.

2.2 Final state $\tau\tau$

In Ref. [4] the ATLAS collaboration reported a search for heavy scalar and pseudoscalar bosons performed with data corresponding to Run 2 of the LHC, with an integrated luminosity of 139 fb^{-1} at a center-of-mass energy of $\sqrt{s} = 13 \text{ TeV}$. The search for heavy resonances was performed within the mass range $0.2 - 2.5 \text{ TeV}$, in the $\tau^+\tau^-$ decay channel. The relevant data for this work is presented in plots of $\sigma_{bb} \times BR_{\tau\tau}$ vs $\sigma_{gg} \times BR_{\tau\tau}$, that show ellipses for one and two standard deviations containing the observed value at the center. For a mass of 400 GeV the SM scenario lies more than two standard deviations away from the observed value. In this work we demand $\sigma \times BR$ lying within the area contended by the 1σ ellipses (excepted where explicitly stated).

2.3 Final state $b\bar{b}$

The CMS collaboration has searched for Higgs bosons decaying into a bottom-antibottom quark pair accompanied by at least one additional bottom-quark, with data corresponding to a center-of-mass energy of 13 TeV and an integrated luminosity of 35.7 fb^{-1} , [10]. The analysis considered scalar and pseudoscalar bosons with masses ranging from 300 to 1300 GeV, finding no significant deviation from the SM. An upper limit for the cross section times branching fraction is reported: $\sigma_{bb} \times BR_{bb} = 5.7 \text{ pb}$ at 95% confidence level (CL), for a mass of 400 GeV.

¹We are using the same notation as Ref. [3] in this subsection.

2.4 Final state $t\bar{t}t\bar{t}$

Another decay channel of interest for the present work consists on the decay of the pseudoscalar boson into four tops. We consider the result reported in Ref. [14] by the ATLAS collaboration, where a production cross section of two pairs top-antitop was found to be 24_{-6}^{+7} fb. Interestingly, notice that this value is roughly two standard deviations above the SM prediction.

2.5 Final state Zh

A pseudoscalar boson decaying into a Z boson and a neutral SM Higgs boson has been probed by the ATLAS and CMS collaborations in multiple searches, finding no evidence of any significant deviation from the SM background. In the present work we consider the constraints for $\sigma \times BR$ reported by the ATLAS collaboration [9], that sets limits in the gluon fusion and bottom fusion initial states, for a mass of 400 GeV the 95% CL bounds are roughly 0.22 pb and 0.25 pb, respectively.

2.6 Final state $\gamma\gamma$

Searches for new heavy particles decaying into two photons within mass ranges containing 400 GeV have been carried out by the ATLAS and CMS collaborations. No excess has been found by any search and upper limits were set for production cross section times branching ratio.

In Ref. [5] the ATLAS collaboration presented a search for scalar particles decaying via narrow resonances into two photons with masses ranging 65 to 600 GeV, using 20.3 fb^{-1} at $\sqrt{s} = 8$ TeV, having found no evidence for the existence of these particles and setting an upper limit of $\sigma \times BR_{\gamma\gamma} \lesssim 2 - 3 \text{ fb}$ at 95% CL. Another search performed by the ATLAS collaboration is presented in Ref. [7] with an integrated luminosity of 36.7 fb^{-1} at $\sqrt{s} = 13$ TeV. This search included spin-0 particles decaying into a final state consisting on two photons within a mass range of 200 to 2700 GeV. For 400 GeV the upper limit was found to be $2 - 3 \text{ fb}$ at 95% CL. In Ref. [6] the CMS collaboration explored the diphoton mass spectrum from 150 to 850 GeV with an integrated luminosity of 19.7 fb^{-1} , at a center of mass energy of $\sqrt{s} = 8$ TeV. Assuming a total decay width between 0.1 GeV and 40 GeV the CMS collaboration reported an upper limit $\lesssim 4 - 15 \text{ fb}$ at 95% CL.

2.7 Final state VV

The VV final state, with $V = W, Z$, has been explored by the ATLAS and CMS collaborations at the LHC in numerous searches, finding no excesses in any of them.

A search for heavy neutral resonances decaying into a W boson pair was carried out by the ATLAS collaboration in Ref. [26] using a data set corresponding to an integrated luminosity of 36.1 fb^{-1} with a center-of-mass energy of 13 TeV. The search focuses on the decay channel ($WW \rightarrow e\nu\mu\nu$) and provides an upper limit for $\sigma \times BR_{WW}$ as a function of the mass of the resonance, ranging from 200 GeV to 5 TeV. For the analysis various benchmark models were considered, including Higgs-like scalars in different width scenarios. In Ref. [27], the ATLAS collaboration presents a search for heavy resonances decaying into a pair of Z bosons leading to two pairs lepton-antilepton, or two pairs lepton-neutrino, for masses ranging from 200 to 2000 GeV. A similar search was published by the CMS collaboration in the range 130 GeV to 3 TeV [28].

2.8 Final state $Z\gamma$

A search for the Higgs boson and for narrow high mass resonances decaying into $Z\gamma$ is presented by the ATLAS collaboration in Ref. [8] using 36.1 fb^{-1} of pp collisions at $\sqrt{s} = 13 \text{ TeV}$. The search for high mass resonances focuses on spin-0 and spin-2 interpretations. The results are found to be consistent with the SM and upper limits on the production cross section times the branching ratio are reported, varying the observed values between 88 fb and 2.8 fb for masses within 250-2400 GeV in the case of spin-0 resonances.

3 Phenomenology

Considering the experimental hints described in the previous section as a possible sign of new physics at an invariant mass around 400 GeV, we propose initially from a purely phenomenological perspective to do an analysis in which we study the compatibility of some of these hints with the introduction of a new pseudoscalar state a with a mass $m_a = 400 \text{ GeV}$, that interacts solely with 3^{rd} generation charged quarks and leptons, the SM gauge bosons Z , gluons, photons, and H , as:

$$\mathcal{L}_{\text{int}} = \frac{g_{gg}}{4} a G_{\mu\nu} \tilde{G}^{\mu\nu} + \frac{g_{\gamma\gamma}}{4} a F_{\mu\nu} \tilde{F}^{\mu\nu} + g_{Zh} (a \overleftrightarrow{\partial}_\mu h) Z^\mu + i g_t a \bar{t} \gamma^5 t + i g_b a \bar{b} \gamma^5 b + i g_\tau a \bar{\tau} \gamma^5 \tau, \quad (1)$$

with $\tilde{F}^{\mu\nu} = (1/2)\epsilon^{\mu\nu\rho\sigma} F_{\rho\sigma}$ and similarly for $\tilde{G}^{\mu\nu}$, g_t , g_b , g_τ , and g_{Zh} dimensionless couplings, whereas g_{gg} and $g_{\gamma\gamma}$ have dimension of an inverse mass scale, the first ones are expected to be present at tree level, whereas the second ones are expected to be induced at the one-loop level. This is the most general CP-invariant interaction Lagrangian linear in the pseudoscalar state a that can be written up to dimension-5 operators, neglecting pseudoscalar interactions with the kinetic terms of massive electroweak gauge bosons $\tilde{Z}_{\mu\nu} Z^{\mu\nu}$ and $\tilde{W}_{\mu\nu}^\dagger W^{\mu\nu}$ and with $\tilde{F}_{\mu\nu} Z^{\mu\nu}$ that, though they are of the same order as the interaction with photons (1-loop order), for the phenomenology we want to address they turn out to be irrelevant. In fact, due to their connection via electroweak (EW) symmetry, the pseudoscalar coupling to EW massive gauge bosons and to $Z\gamma$ should be similar in nature to the diphoton coupling. Rescaling the photon coupling by the corresponding factors and modifying the decay rates by the appropriate phase spaces we obtain, in the interesting region of couplings, VV and $Z\gamma$ cross sections that are one to two orders of magnitude below the bounds discussed in the previous section.

In order to be able to separate the contribution of possible heavy colored and/or electromagnetically charged beyond the SM (BSM) states to g_{gg} and $g_{\gamma\gamma}$ that have been integrated out from our effective theory, from those of the 3^{rd} generation quarks and leptons, we explicitly write g_{gg} and $g_{\gamma\gamma}$ as,

$$g_{gg} = \frac{3\alpha_s}{12\pi m_t} \times 4.2(x + g_t), \quad g_{\gamma\gamma} = \frac{3\alpha}{2\pi m_t} \times \left(\frac{2}{3}\right)^2 4.2 \left(z + g_t + x \left(\frac{Q_x}{2/3}\right)^2 \right), \quad (2)$$

with $\alpha_s = g_s^2/(4\pi)$ and $\alpha = e^2/(4\pi)$ and where we are already assuming that in Eq. (1), in what concerns the SM quark contributions, only the top quark provides sizable contributions to the loop-induced couplings and we explicitly used that the loop function $A_{1/2}^a(m_a^2/(4m_t^2)) \approx 4.2$ for $m_a = 400 \text{ GeV}$. Furthermore, we parameterize the contributions from heavy BSM states that have been integrated out as coming from vector-like fermions in the fundamental representation of $SU(3)_c$ with EM charge Q_x , whose contribution is accounted by the dimensionless parameter x and a separate BSM contribution from colorless vector-like fermions charged under EM and accounted

by the dimensionless parameter z . These loop contributions are normalized with respect to the top quark contribution such that, for example, in the presence of a color triplet heavy fermion F with EM charge $Q_x = Q_F$, are:

$$x = x_F = \frac{g_F m_t}{m_F} \times \frac{2}{4.2}, \quad (3)$$

where we used $A_{1/2}^a(m_a^2/(4m_F^2)) \approx 2$ for $m_F \gg m_a$, and g_F is the vector-like coupling of a to the heavy fermion F . Analogously, for a colorless vector-like fermion E with EM charge Q_E we would obtain,

$$z = z_E = \frac{1}{3} \left(\frac{Q_E}{2/3} \right)^2 \frac{g_E m_t}{m_E} \times \frac{2}{4.2}. \quad (4)$$

We restrict ourselves to the case in which the pseudoscalar behaves as a narrow resonance, narrow width approximation (NWA), with a total width $\Gamma_a/m_a \leq 8\%$. The dominant 2-body partial decay widths for a take the form,

$$\Gamma_{a \rightarrow f\bar{f}} = N_c \frac{g_f^2 m_a}{8\pi} \sqrt{1 - 4 \frac{m_f^2}{m_a^2}}, \quad (5)$$

$$\Gamma_{a \rightarrow Zh} = \frac{g_{Zh}^2 m_a^3}{16\pi m_Z^2} \left[1 + \left(\frac{m_h^2 - m_Z^2}{m_a^2} \right)^2 - 2 \left(\frac{m_h^2 + m_Z^2}{m_a^2} \right) \right]^{3/2}, \quad (6)$$

$$\Gamma_{a \rightarrow gg} = \frac{g_{gg}^2 m_a^3}{8\pi}, \quad (7)$$

$$\Gamma_{a \rightarrow \gamma\gamma} = \frac{g_{\gamma\gamma}^2 m_a^3}{8\pi}, \quad (8)$$

where f represents the fermions of interest, $f = t, b, \tau$ and $N_c = 3$ for $f = t, b$ and $N_c = 1$ for τ .

In what respects the production of the pseudoscalar, the main channels are gluon and bottom fusion. Following Ref. [29], the hadronic production cross section from parton pairs $\mathcal{P}\bar{\mathcal{P}}$ at an energy \sqrt{s} can be written as,

$$\sigma(pp \rightarrow a) = \frac{1}{s \times m_a} \sum_{\mathcal{P}} C_{\mathcal{P}\bar{\mathcal{P}}} \Gamma_{a \rightarrow \mathcal{P}\bar{\mathcal{P}}}. \quad (9)$$

For the LHC at $\sqrt{s} = 8, 13$ TeV, considering only couplings to gluons and bottom-quarks, we obtain the following:

\sqrt{s}	C_{gg}	$C_{b\bar{b}}$
8 TeV	4592	29
13 TeV	40187	278

The typical values that we find for the production cross sections at the LHC for $\sqrt{s} = 13$ TeV that are consistent with the experimental hints are ~ 20 pb and ~ 10 pb for gluon and bottom fusion, respectively.

Having all these elements at hand, we can calculate under the NWA, the contribution of a to the different final states that either show a possible hint of BSM physics or otherwise put a constraint on the couplings of the pseudoscalar to SM particles. We do this in the following section and comment on our findings. In particular we focus on the cases in which there could be a UV contribution to the gluonic operator $x \neq 0$ and when such contribution vanishes, $x = 0$.

4 Numerical results

In this section we study the cross sections of the different production modes of the 400-GeV pseudoscalar, taking into account their dominant decay channels, as a function of two parameters at a time, fixing the rest of the parameters to two benchmark points, one with $x = 0$ and another one with $x \neq 0$, defined as follows:

- $g_t = 0.78, g_b = 0.39, g_\tau = 0.04, x = 0,$
- $g_t = 0.7, g_b = 0.37, g_\tau = 0.04, x = 0.13.$

All the cross sections have been computed with the expressions detailed in the previous section, except the $t\bar{t}\bar{t}$ production, which has been calculated with `MadGraph_aMC@NLO 2.5.2` [30] at leading order. For the pseudoscalar productions via gluon fusion and in association with bottom-quarks we have considered K -factors of 2 [31] and 1.24 [32], respectively, while a K -factor of 1.27 [33], with a 20% uncertainty, has been used for $t\bar{t}\bar{t}$ production. Likewise, for each final cross section we consider 1σ uncertainties, also detailed in Section 2. We present the results as contour plots of the different cross sections as a function of a pair of couplings, and each contour line is labeled with the corresponding cross-section value at $\pm 1\sigma$. The red shaded areas correspond to values of the cross sections lower than their reference values subtracting their uncertainty of 1σ , and the blue ones to higher than these reference values plus 1σ . In the case of the ditau channel, we demand consistency at the 1σ level with the experimental measurements (given by an ellipse in the gluon and bottom fusion channels, see Section 2). Therefore, both blue and red shaded areas are excluded by data, and only the white area would be allowed by the LHC experimental measurements and consistent with the possible hints of new physics. Recall also that the only channels that show slight excesses or deviations from the SM predictions are $t\bar{t}$ and $\tau^+\tau^-$, as well as 4-tops although in this case a new pseudoscalar is not particularly favored, while the other channels only impose exclusion limits on the total cross sections at 95% CL. In addition, it is important to note that the channels that are not shown in the following contour plots are due to the fact that they impose softer constraints on our parameter space. In particular, we find that the coupling to a Z and a Higgs is restricted to: $g_{Zh} \lesssim 0.03$, roughly independently of the other couplings, while the new physics contribution to diphotons, called z , shows a stronger dependence on g_t and x , with larger values allowed for smaller g_t and x : $z \lesssim 1.2$ for $g_t = 0.7$ and $x = 0$, and smaller values for larger g_t and x : $z \lesssim 0.5$ for $g_t = 0.78$ and $x = 0.13$. Neither g_{Zh} nor z determine the shape of the white regions in the plots we show.

Concerning the branching ratios of the dominant decay channels of the 400-GeV pseudoscalar, we find that for the parameter region consistent with the experimental measurements, they are dominated by either ditops or dibottoms since we find that the pseudoscalar coupling to ditops is large, but more interestingly the consistency with measurements implies a large coupling to dibottoms, up to 30 times the Higgs bottom-quark Yukawa coupling. For the benchmark scenario with $x = 0$, the maximum value for $\text{BR}(a \rightarrow t\bar{t})$ allowed by our analysis is 0.970, the minimum one is 0.270 and the average value is 0.675, while the maximum value for $\text{BR}(a \rightarrow b\bar{b})$ is 0.726, the minimum one is 0.022 and the average value is 0.319. On the other hand, within the benchmark scenario with $x = 0.13$, the maximum, minimum, and average values allowed by our analysis for the $t\bar{t}$ ($b\bar{b}$) decay modes are 0.806, 0.541, and 0.696 (0.450, 0.187, and 0.296), respectively. Notice also that the contribution of the bottom-quark loop to the production of the 400-GeV pseudoscalar via gluon fusion, for the favored values of the g_b and g_t couplings, is of order 6-8% compared to that of the top-quark loop. ²

²Also as comparison, for the production of the SM Higgs boson, the b -quark contribution to the gluon-fusion

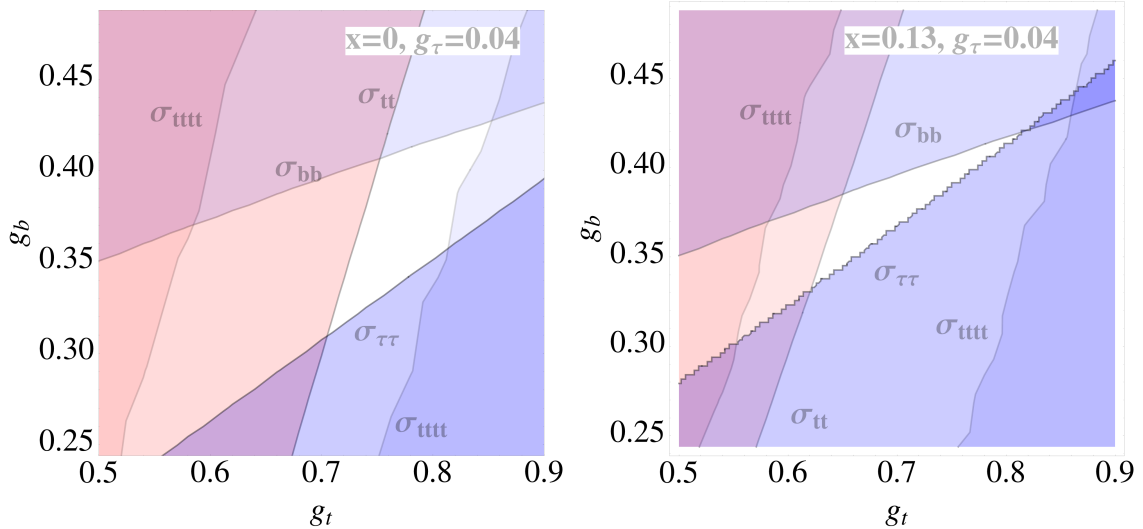


Figure 1: Production cross-section predictions of relevant 400-GeV pseudoscalar channels with 1σ uncertainties of in the $[g_t, g_b]$ plane, with $x = 0$ (left panel) and $x = 0.13$ (right panel). In both plots g_τ is fixed to 0.04. Each contour line is labeled with the 1σ cross-section value of the corresponding considered channel. Blue and red shaded areas are excluded by data.

In the left panel of Fig. 1 we show the values of the cross sections with an uncertainty of 1σ of the channels $t\bar{t}$, $t\bar{t}t\bar{t}$, and $\tau^+\tau^-$ in the $[g_t, g_b]$ plane with $x = 0$ and $g_\tau = 0.04$. Each contour line is labeled with the corresponding value at 1σ , marking the blue ($+1\sigma$) and red (-1σ) shaded areas that are excluded by data. Therefore, only g_t values ranging from about 0.7 to 0.85 would be allowed by the LHC experimental measurements, provided that g_b is more or less within the range $[0.28, 0.4]$. In this favored region the width varies 4-6% with respect to the mass, dominated by the $t\bar{t}$ decay channel, and the main branching fractions vary among these values: $\text{BR}(a \rightarrow t\bar{t}) \sim 0.6-0.8$, $\text{BR}(a \rightarrow b\bar{b}) \sim 0.2-0.4$, $\text{BR}(a \rightarrow \tau^+\tau^-) \sim 0.001$, and $\text{BR}(a \rightarrow gg) \sim 0.035-0.045$. These latter values of $\text{BR}(a \rightarrow gg)$ hardly change as a functions of the couplings considered and will not be shown again. The right panel of Fig. 1 is devoted to same analysis but switching on the coupling x , with a value of 0.13. Since the coupling of the pseudoscalar to gluons is now contributing to the $t\bar{t}$ channel, the constraints on g_t are softer and this coupling can take lower values, close to 0.6. The maximum g_t values are also reduced, up to approximately 0.8. The range of allowed values of g_b is also reduced, from values around from 0.32 to 0.37. In this case the width varies 3.5-6% and the branching ratios of the dominant channels are $\text{BR}(a \rightarrow t\bar{t}) \sim 0.55-0.75$, $\text{BR}(a \rightarrow b\bar{b}) \sim 0.25-0.45$, and $\text{BR}(a \rightarrow \tau^+\tau^-) \sim 0.001$. The reduction in the white area when comparing the figure on the left with $x = 0$ with the right one at $x = 0.13$ is provided by the increased constraint in the ditau channel since in fact there is a reduction in the constraint from the ditop channel which would have naively provided a larger white area. However this increment in the ditau constraint can be understood by looking on the right plot of Fig. 2 where we see that the ditau ellipse allows larger values of g_t at $x = 0$ than at $x = 0.13$, which is sensible since both x and g_t contribute to the gluon fusion diagram that enters in the ditau channel. Coming back to Fig. 1, the preferred values for g_t and g_b , which we have calculated with our effective model, compatible with the ATLAS and CMS experimental measurements, lie in the white areas and therefore are able to explain the new physics hints while at the same time are consistent with the data at 68% CL.

is approximately 3-4% that of the t -quark, besides the coupling of the Higgs to bottoms is much smaller than the 400-GeV pseudoscalar one.

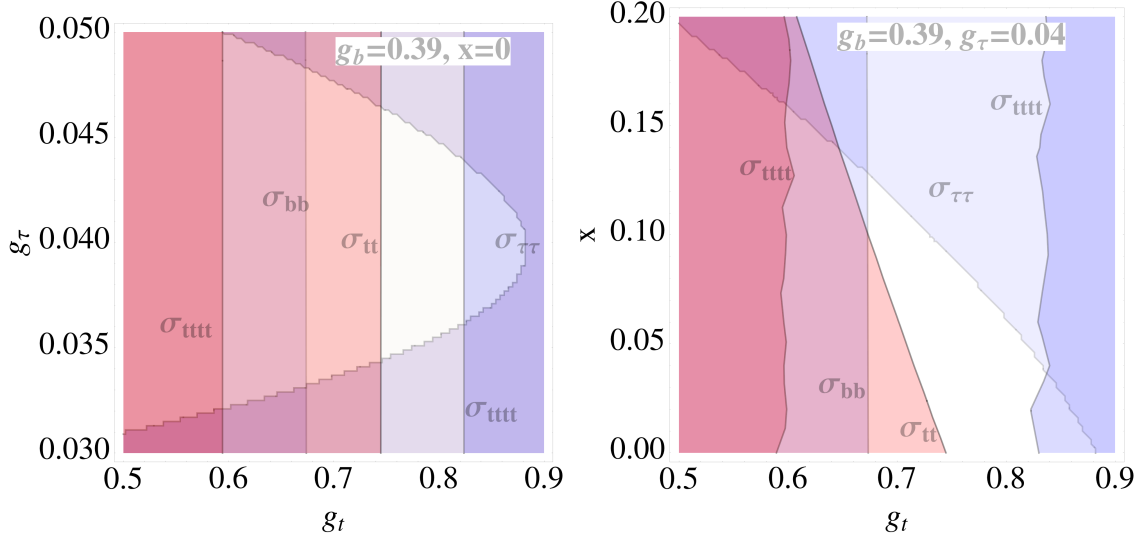


Figure 2: Production cross-section predictions of relevant 400-GeV pseudoscalar channels with 1σ uncertainties in the $[g_t, g_\tau]$ (with $x = 0$ and $g_b = 0.39$) and $[g_t, x]$ ($g_\tau = 0.04$ and $g_b = 0.39$) planes, left and right panels, respectively. Each contour line is labeled with the 1σ cross-section value of the corresponding considered channel. Blue and red shaded areas are excluded by data.

Left panel of Fig. 2 is dedicated to the pseudoscalar cross-section predictions in the $[g_t, g_\tau]$ plane, with $x = 0$ and $g_b = 0.39$. Contour lines label the values of these cross sections with 1σ uncertainty, indicating the blue and red shaded areas not allowed by data. The parameter space region allowed by data is centered at $g_t \sim 0.78$ and $g_\tau \sim 0.040$, with g_t varying between 0.74 and 0.82, and g_τ between 0.033 and 0.047, approximately. In the favored region the width varies 5.5-6% with respect to the mass, increasing mainly with g_t , since the branching fractions to τ -lepton pairs is small. The main branching fractions take the following values: $\text{BR}(a \rightarrow t\bar{t}) \sim 0.65\text{-}0.7$, $\text{BR}(a \rightarrow b\bar{b}) \sim 0.3\text{-}0.35$, and $\text{BR}(a \rightarrow \tau^+\tau^-) \sim 0.001\text{-}0.002$. It is important to remark here that these not-excluded values of g_t are in accordance with the allowed values in the $[g_t, g_b]$ plane of Fig. 1. Contrary to these contour plots, once the the restrictions from the other channels are accomplished, the $b\bar{b}$ channel does not impose any restriction on the parameter space of the $[g_t, g_\tau]$ plane, with the values set as we have indicated for the rest of the couplings, and the most restrictive channels are only $t\bar{t}$, $\tau^+\tau^-$, and $t\bar{t}t\bar{t}$.

In the right panel of Fig. 2 we show the values of the cross sections with an uncertainty of 1σ of the channels $t\bar{t}$, $t\bar{t}t\bar{t}$, and $\tau^+\tau^-$ ($gg \rightarrow a \rightarrow \tau^+\tau^-$) in the $[g_t, x]$ plane. Only g_t values ranging from about 0.68 to 0.83 would be allowed by the LHC experimental measurements, provided that x is less than 0.13. In this favored region the width varies 4.5-6% with respect to the mass, dominated by the $t\bar{t}$ decay channel, since the branching ratio to gluons is small and the branching ratios of the dominant decay channels are $\text{BR}(a \rightarrow t\bar{t}) \sim 0.61\text{-}0.68$, $\text{BR}(a \rightarrow b\bar{b}) \sim 0.31\text{-}0.38$, and $\text{BR}(a \rightarrow \tau^+\tau^-) \sim 0.001$. In this plane, the $b\bar{b}$ channel comes back into play by excluding a small portion of the parameter space that $t\bar{t}$, $\tau^+\tau^-$, and $t\bar{t}t\bar{t}$ allowed.

In the left panel of Fig. 3 the 1σ cross-section values of the $t\bar{t}$, $t\bar{t}t\bar{t}$, and $b\bar{b}b\bar{b}$ channels are displayed in the $[g_\tau, g_b]$ plane. The allowed values of g_τ (white area) vary between 0.035 and 0.046, depending on the value of g_b , which is constrained to the range $[0.37, 0.42]$. In the favored region the width varies 5.5-6% with respect to the mass, increasing mainly with g_b , since the branching ratio to $\tau^+\tau^-$ is small. The branching fraction of the dominant channels are here $\text{BR}(a \rightarrow t\bar{t}) \sim 0.65\text{-}0.70$, $\text{BR}(a \rightarrow b\bar{b}) \sim 0.3\text{-}0.35$, and $\text{BR}(a \rightarrow \tau^+\tau^-) \sim 0.001$. These values of g_τ correspond to

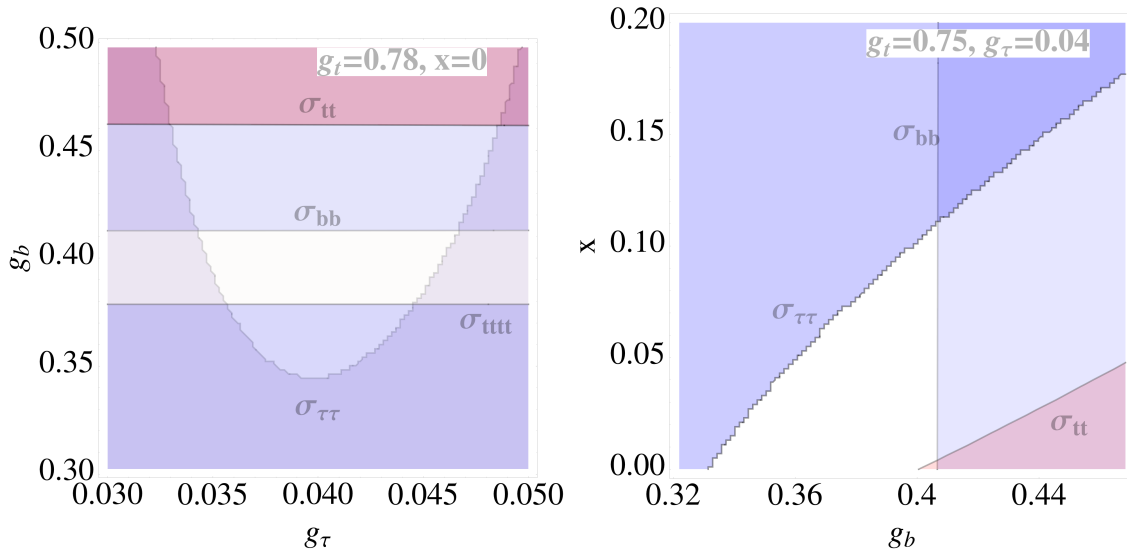


Figure 3: Production cross-section predictions of relevant 400-GeV pseudoscalar channels with 1σ uncertainties in the $[g_\tau, g_b]$ (with $g_t = 0.78$ and $x = 0$) and $[g_b, x]$ (with $g_t = 0.75$ and $g_\tau = 0.04$) planes, left and right, respectively. Each contour line is labeled with the 1σ cross-section value of the considered corresponding channel. Blue and red shaded areas are excluded by data.

those allowed in the left panel of Fig. 2, which indicate a good agreement of these data at 68% CL.

The contour lines of the cross sections of the $t\bar{t}$, $b\bar{b}$, and $\tau^+\tau^-$ channels, with 1σ of uncertainty, are shown in the right panel of Fig. 3 in the $[g_b, x]$ plane. Allowed values of g_b vary between 0.33 and 0.4, while x can reach allowed values up to 0.10, depending strongly on g_b . In the favored region the width varies 4.5-5.5% with respect to the mass, increasing mainly with g_b , since the branching fraction to gluons is small. The dominant branching ratios are in this case $\text{BR}(a \rightarrow t\bar{t}) \sim 0.64-0.72$, $\text{BR}(a \rightarrow b\bar{b}) \sim 0.28-0.36$, and $\text{BR}(a \rightarrow \tau^+\tau^-) \sim 0.001$. Again, the values of x and g_b are in agreement with the allowed values of Figs. 1 and 2.

One significant conclusion is that the most restrictive channels are $t\bar{t}$, $t\bar{t}t\bar{t}$, and $\tau^+\tau^-$, in which the production of the pseudoscalar and/or its decays are governed by g_t , together with the $b\bar{b}$ channel when the values of g_b are significant and competitive with respect to those of g_t . Recall also that in the scenario with $x = 0.13$, the bounds imposed by $t\bar{t}t\bar{t}$ channel are lower than the other channels.

Finally, we find it important to keep in mind that the white areas of the six plots shown in this section are compatible with each other and show the allowed-by-data values for each of the effective couplings of a 400 GeV pseudoscalar that can produce the slight excesses in $t\bar{t}$ and $\tau^+\tau^-$ reported by CMS and ATLAS, respectively.

5 UV completions

In this section we describe several models and analyze whether they can reproduce the phenomenology of the previous section. We start with 2HDMs, finding that usually they can not pass the constraints from flavor violating decays. Then we consider models containing a composite pseudoscalar singlet, and study the case where this state is a pNGB.

5.1 Two Higgs doublet models

These models contain a neutral pseudoscalar that could reproduce the collider phenomenology. In models of Type-I, II, III and IV the couplings with the SM fermions are proportional to the SM Yukawa coupling, up to the factor t_β or its inverse, with t_β being defined by the ratio of the vacuum expectation values (vev) of both neutral doublets. In Type-I models all the couplings are given by $\pm t_\beta^{-1}$, in units of the SM Yukawa. In Type-II, up-quark couplings are given by t_β^{-1} , whereas down-quarks and charged leptons are given by t_β . In Type-III (also on L 2HDM), quarks have a factor $\pm t_\beta^{-1}$ and charged leptons t_β . In Type-IV (also in F 2HDM), up-quarks and charged leptons have a factor $\pm t_\beta^{-1}$ and down-quarks a factor t_β . These structures of couplings cannot accommodate the excesses.

A generalization for the couplings in the Higgs sector of a 2HDM has been considered in Ref. [16] that allow to enhance the interactions with up- or down-type quarks, while suppressing flavor changing neutral currents via flavor alignment. The authors refer to this framework as Spontaneous Flavor Violation (SFV). Particularly interesting for our study is the case of up-type SFV 2HDM, where in the mass basis the up-quark diagonal Yukawa matrix is rescaled by a real parameter ξ , whereas each down-type Yukawa is rescaled by an independent factor: κ_i , namely: $Y_u = \text{diag}(y_u, y_c, y_t) \rightarrow \xi Y_u$ and $Y_d = \text{diag}(y_d, y_s, y_b) \rightarrow \text{diag}(\kappa_d, \kappa_s, \kappa_b)$. A similar framework corresponds to the down-type SFV 2HDM, exchanging the role of up- and down-type quarks. In the sector of charged leptons: $Y_\ell = \text{diag}(y_e, y_\mu, y_\tau) \rightarrow \xi_\ell Y_\ell$. The new parameters are independent, and can be suitably chosen to reproduce the collider phenomenology we wish to describe.

The problem arises given that this model gets strong constraints from flavor physics. Since the neutral Yukawa couplings are aligned, flavor violation requires the presence of a charged Higgs boson. For large κ_b this state gives contributions to C_7^{bs} at 1-loop, inducing $B \rightarrow s\gamma$. Following Ref. [16], for the values of ξ and κ_b that can fit the results of Section 4, we obtain a strong lower bound on the mass of the charged Higgs: $m_H \gtrsim 3.4$ TeV. But in 2HDMs m_H and m_A are related by $m_A^2 = m_H^2 + v^2(\lambda_4 - \lambda_5)/2$, with $V \supset \lambda_4(H_2^\dagger H_1)(H_1^\dagger H_2) + \lambda_5(H_1^\dagger H_2)/2$, thus one would have to require $(\lambda_4 - \lambda_5)/2 \sim \mathcal{O}(100)$ for $m_A \sim 400$ GeV, losing perturbative control of the theory.

5.2 Composite models with a pseudoscalar singlet

An interesting possibility is the presence of a new strongly interacting sector, with a mass gap at an infrared scale of order few TeV, that leads to bound states, to which we will refer as resonances, one of them being a pseudoscalar. We will consider the case where the pseudoscalar is a singlet under the SM gauge symmetry. Moreover, we will take it as a composite NGB of the new sector, generated by the spontaneous breaking of a global symmetry, such that it can be lighter than the rest of the resonances. In this case the shift symmetry of the NGB singlet forbids a potential, making this state massless, but if the symmetry is explicitly broken by the interactions with the SM, a potential is generated at radiative level. The SM gauge interactions can give this explicit breaking of the global symmetry, the interactions with the SM fermions can also do that, the latter being model dependent. One of the most popular examples for the interactions with fermions is partial compositeness, where at a high UV scale $\Lambda_{\text{UV}} \gg \text{TeV}$ linear interactions of the SM fermions and the composite operators are generated: $\mathcal{L}_{\text{UV}} = \lambda \bar{\psi}^{\text{SM}} \mathcal{O}$.³ The shift symmetry can also be broken by anomalous interactions with the SM gauge fields, as in the case of the η' of QCD, or by anomalies in the new sector, that are independent from the first ones. [34, 35]

It is interesting to consider that also the Higgs arises as a pNGB [17–23], obtaining an explanation for its mass being smaller than the masses of the other resonances, although tuning is still

³ Λ_{UV} can be, for example, of order M_{Pl} or M_{GUT} .

required [36]. Scenarios with the pseudoscalar singlet and the Higgs being composite pNGBs have been considered, for example, in Refs. [24, 25, 29, 37], giving estimates of the potential and couplings with the SM sector, as well as building specific realizations. In the following we will describe some general properties of a pseudoscalar singlet that is a composite pNGB, and in the next subsections we will consider some realizations of these ideas for the hints at 400 GeV.

In the simplest example the resonances of the strongly interacting sector are determined by one mass scale, namely, the decay constant of the NGBs, f , that sets the scales of their self-interactions, and one coupling, g_* , that characterizes all the interactions between resonances. These couplings can be thought in analogy with f_π and g_ρ for the QCD mesons. We will consider $1 \ll g_* \ll 4\pi$ and the resonance's masses given by $m_* = g_* f$. There can be departures from this very simplified picture, for example if the NGBs arise from a non-simple group their decay constants can be different: f_H for the Higgs and f_P for the singlet, there can also be different couplings and deviations from the estimate of m_* . For simplicity we will assume the one scale and one coupling approach, except where explicitly stated.

For the interactions with fermions we will consider $\Lambda_{UV} \gg m_*$ and approximate scale invariance in a large window of energy, such that the running of the linear coupling λ is driven by the anomalous dimension of \mathcal{O} , leading to an exponentially suppressed coupling for an irrelevant operator and to $\lambda \sim g_*$ for a relevant one [38]. At energies of order m_* the linear interactions lead to mixing of the elementary and composite fermions, such that the massless fermions, before EW symmetry breaking, are partially composite, with a degree of compositeness $\epsilon_\psi \sim \lambda_\psi(m_*)/g_*$. The Yukawa couplings are modulated by ϵ as:

$$y_\psi \sim \epsilon_{\psi_L} g_* \epsilon_{\psi_R} . \quad (10)$$

In the case of three generations of resonances, ϵ and g_* are squared matrices of dimension three.

When the breaking of the shift symmetry is dominated by partial compositeness, the mass of the (pseudo) scalar can be estimated as:

$$m_h^2 \sim N_c y_t^2 \frac{g_*^2}{(4\pi)^2} v^2 ; \quad m_P^2 \sim N_c y_t^2 \frac{g_*^2}{(4\pi)^2} f^2 . \quad (11)$$

The separation between v and f typically requires a tuning of order $\xi \equiv v^2/f^2$, and allows a splitting between m_h and m_P . For $f \simeq 800$ GeV one can obtain $m_P \simeq 400$ GeV, although these estimations are up to factors of $\mathcal{O}(1)$.⁴

At energies below m_* , one gets a theory with the SM fields and the pNGB H and P . The P interactions with SM fermions and gauge bosons require at least dimension-5 operators:

$$\mathcal{L}_{\text{eff}} \supset \frac{g_{PAA}}{\Lambda} P A_{\mu\nu} \tilde{A}^{\mu\nu} + i \frac{g_{P\psi\psi'}}{\Lambda} P \bar{\psi}_L H \psi'_R , \quad (12)$$

where $A_{\mu\nu}$ stands for a generic SM gauge field strength tensor, ψ_L and ψ'_R are SM fermions and Λ is the scale at which these operators are generated, that for simplicity was written to be the same for all the operators. One could also include terms as $\partial_\mu P \bar{\psi} \gamma^\mu \psi$, however they can be absorbed in the Yukawa and anomalous terms after field redefinitions [39].

The coupling with the gauge bosons, $PA\tilde{A}$, breaks the shift symmetry of the NGBs, requiring either insertions of the fermion mixing that explicitly break the symmetry, or an anomalous breaking, generating topological terms, as the Wess-Zumino-Witten term [40, 41]⁵. To leading order in $1/f_P$ one gets:

$$\mathcal{L}_{\text{eff}} \supset \frac{P}{16\pi^2 f_P} \left(c_s g_s^2 G\tilde{G} + c_W g^2 W\tilde{W} + c_B g'^2 B\tilde{B} \right) . \quad (13)$$

⁴Contributions to the pseudoscalar mass from anomalies in the new sector can be estimated as $m_P^2 \sim \tilde{N}_f g_*^2 / (4\pi)^2 f^2$, with \tilde{N}_f determined by the number of fermions responsible for the anomaly.

⁵See also [42] for a discussion of topological terms.

The coefficients can be estimated as:

$$c_i|_{\text{pc}} \sim N_c \frac{y_\psi^2}{g_*^2}, \quad c_i|_{\text{anom}} \sim N_f. \quad (14)$$

In both cases the interaction is generated at loop level, in the first case it is modulated by the Yukawa couplings of the SM fermions, whereas in the second case c_i measures the number of fermions N_f generating the anomaly. Rewriting Eq. (13) in the basis of mass eigenstates, one obtains the interaction with photons, with coefficient $e^2(c_W + c_B)/(16\pi^2 f_P)$.

As we will show in the next subsections, it is interesting to write $g_{P\psi\psi}$ as function of y_ψ , the matrix of Yukawa coupling of the Higgs, in the following form:

$$\frac{g_{P\psi\psi}}{\Lambda} = \frac{A_\psi y_\psi}{f_P} + \frac{y_\psi B_\psi}{f_P}, \quad (15)$$

where A_ψ and B_ψ are 3×3 matrices, determined by the embedding of the Left- and Right-handed fermions, respectively. After rotation of the SM fermions to the mass basis, $\psi_{L/R} \rightarrow U_{L/R}\psi_{L/R}$, one gets:

$$\frac{g_{P\psi\psi}}{\Lambda} \rightarrow U_L^\dagger A_\psi U_L \frac{m_\psi}{f_P} + \frac{m_\psi}{f_P} U_R^\dagger B_\psi U_R, \quad (16)$$

where m_ψ is the diagonal fermion mass matrix. As expected, for A and B proportional to the identity the couplings are aligned with the masses, whereas in other cases they are not and lead to flavor transitions.

A better determination of the flavor violating couplings requires assumptions about the flavor of the new sector. We will consider the case of flavor anarchy [43], where the couplings between fermionic and pseudo/scalar resonances are given by matrices with all the coefficients of order g_* , such that flavor transitions between resonances have no suppression. It is well known that in this case bounds from flavor changing neutral currents (FCNC) require $m_* \gtrsim 10 - 20$ TeV [43, 44].

In anarchic partial compositeness the size of the coefficients of the rotation matrices are determined by the degree of compositeness. Ordering the flavors by increasing mixing, leads to $(U_{\psi_L})_{ij} \sim \epsilon_{q\psi}^i / \epsilon_{q\psi}^j$ and $(U_{\psi_R})_{ij} \sim \epsilon_\psi^i / \epsilon_\psi^j$, with $i < j$.

For quarks, assuming that $(U_{u_L})_{ij} \sim (U_{d_L})_{ij}$ ⁶, we get:

$$\epsilon_q^i \sim (V_{\text{CKM}})_{i3} \epsilon_q^3, \quad i < 3, \quad (17)$$

$$\epsilon_\psi^i \sim \frac{m_\psi^i}{v} \frac{1}{(V_{\text{CKM}})_{i3} g_* \epsilon_q^3}, \quad \psi = u, d. \quad (18)$$

These equations determine the degree of compositeness of the chiral quarks in terms of physical parameters as the CKM angles and masses. The only parameters that are not determined are ϵ_q^3 and g_* , although the masses give lower bounds for ϵ_q^3 when the right mixings are saturated, $\epsilon_q^3 \gtrsim 1/g_*$.

Similar estimates can be made for leptons, although in this case U_{PMNS} depends on the realization of neutrino masses. Assuming that the large mixing angles of the PMNS matrix are generated in the neutrino sector, bounds from flavor violation in the lepton sector are minimized around the Left-Right symmetric limit, $\epsilon_l^i \sim \epsilon_e^i$ [45], leading to:

$$\epsilon_{l,e}^i = \sqrt{\frac{m_\ell^i}{g_* v}}. \quad (19)$$

	u	d	e
$(U_R)_{12}$	$\frac{m_u}{m_c \lambda_C} \sim 0.01$	$\frac{m_d}{m_s \lambda_C} \sim 0.2$	$\sqrt{\frac{m_e}{m_\mu}} \sim 0.07$
$(U_R)_{23}$	$\frac{m_c}{m_t \lambda_C^2} \sim 0.07$	$\frac{m_s}{m_b \lambda_C^2} \sim 0.4$	$\sqrt{\frac{m_\mu}{m_\tau}} \sim 0.2$
$(U_R)_{13}$	$\frac{m_u}{m_t \lambda_C^3} \sim 7 \times 10^{-4}$	$\frac{m_d}{m_b \lambda_C^3} \sim 0.08$	$\sqrt{\frac{m_e}{m_\tau}} \sim 0.02$

Table 1: Estimates of coefficients of unitary Right-handed matrices using partial compositeness, taking the masses at the TeV scale.

In this framework the coefficients of the rotation matrices can be estimated as in Table 1.

The integration of P leads to FCNC with the four fermion interactions [24],

$$\mathcal{L}_{\text{eff}} = C_\psi^{ijkl} (\bar{\psi}_L^i \psi_R^j) (\bar{\psi}_L^k \psi_R^l), \quad (20)$$

$$C_\psi^{ijkl} = g_{P\psi^i\psi^j} g_{P\psi^k\psi^l} \frac{v^2}{2\Lambda^2} \frac{1}{m_P^2}. \quad (21)$$

The $\Delta F = 2$ bounds from meson mixing give constraints on the size of the flavor violating coefficients, $C_2^{ij} = C_\psi^{ijij}$.

There can also be dimension-5 operators with covariant derivatives, that can violate flavor, as $P\bar{\psi}_{L/R} i \not{D} \gamma^5 \psi_{L/R}$. These operators can be rewritten in terms of $P\bar{\psi}_L \gamma^5 H \psi'_R$ and its hermitian conjugate after field redefinitions [46, 47].

5.3 A model with P from $\text{SO}(6)/\text{SO}(5)$

Refs. [24, 25] have considered the spontaneous breaking $\text{SO}(6)$ to $\text{SO}(5)$, that delivers five pNGBs transforming as $\mathbf{5}$ $\text{SO}(5)$. By using that $\text{SO}(4) \sim \text{SU}(2)_L \times \text{SU}(2)_R$, under this group $\mathbf{5} \sim (\mathbf{2}, \mathbf{2}) \oplus (\mathbf{1}, \mathbf{1})$, leading to a model with custodial symmetry that generates a Higgs and a pseudoscalar singlet. An extra conserved $\text{U}(1)_X$ factor must be added to accommodate the hypercharge of the SM fermions, with $Y = T_R^3 + X$.

The NGB unitary matrix is given by:

$$U = \exp(i\sqrt{2}\Pi/f); \quad \Pi = h^{\hat{a}} T^{\hat{a}} + P T_P; \quad (22)$$

where $T^{\hat{a}}$ and T_P are the broken generators associated to the Higgs and the pseudoscalar.

To determine the interactions of the NGBs with the SM fermions one has to choose the representations of the fermionic composite operators \mathcal{O} that mix with the elementary fermions. To avoid explicit breaking of the SM gauge symmetry, these $\text{SO}(6)$ representations, when decomposed under the SM gauge symmetry, must contain multiplets transforming as the SM fermions, or in other words: the EW representations of the SM fermions are embedded into representations of $\text{SO}(6) \times \text{U}(1)_X$. These embeddings are not unique, and the phenomenology of P , in many aspects, depends strongly on this choice. We will consider the following embeddings:

$$\mathcal{O}_{q^u}, \mathcal{O}_u \sim \mathbf{6}_{2/3}, \quad \mathcal{O}_{q^d}, \mathcal{O}_d \sim \mathbf{6}_{-1/3}, \quad \psi_l, \psi_e \sim \mathbf{6}_{-1}. \quad (23)$$

The presence of two embeddings for q : q^u and q^d , means that it interacts linearly with two different operators: $\mathcal{L} \supset \bar{q}(\lambda_{q^u} \mathcal{O}_{q^u} + \lambda_{q^d} \mathcal{O}_{q^d})$. $\mathbf{6}$ is the smallest dimensional representation that allows to

⁶This assumption is not necessary, since the condition is $U_{u_L}^\dagger U_{d_L} = V_{CKM}$, it is a simple hypothesis under which we can estimate the mixings. It is also possible to mix the elementary fermions with more than one composite operator, leading to less trivial situations.

protect the $Zb_L\bar{b}_L$ coupling, that demands embedding q in a $(\mathbf{2}, \mathbf{2})_{2/3}$ of $\text{SO}(4)\sim\text{U}(1)_X$ [48]. u is embedded in the same representation, but since there are two $\text{SO}(4)$ singlets $\mathbf{6} \sim \mathbf{5} \oplus \mathbf{1} \sim (\mathbf{2}, \mathbf{2}) \oplus (\mathbf{1}, \mathbf{1}) \oplus (\mathbf{1}, \mathbf{1})$, there is a free parameter $c_u \equiv \cos\theta_u$ that determines the projection over the $\text{SO}(5)$ singlet, whereas $s_u \equiv \sin\theta_u$ determines its projection over the $\mathbf{5}$, in fact there is one θ_u for each generation. Since $\mathbf{6}_{2/3}$ does not contain a $-1/3$ singlet, the down sector is embedded in a $\mathbf{6}_{-1/3}$, with a new parameter θ_d , similar to the up sector. Finally the leptons are embedded in a $\mathbf{6}_{-1}$, with a θ_e for the lepton singlet.

Since the SM fermions do not fill the embeddings, the linear interactions that lead to partial compositeness explicitly break the global symmetry and generate a potential for the NGBs, which coefficients can be estimated as we did for the quadratic ones in Eq. (11) [25].

We assume that at low energies, of order few to ten TeV, the strong dynamics generates resonances that mix with the elementary fermions. Integrating them one obtains to leading order:

$$\mathcal{L}_{\text{eff}} \supset \sum_{\psi=u,d,\ell} \bar{\psi}_L \frac{m_\psi}{v} \left(h + i \frac{P}{f} \cot\psi \right) \psi_R + \text{h.c.} , \quad (24)$$

where generation indices are understood, such that $\cot\psi$ is a matrix in the generation space:

$$\cot\psi = \text{Diag}(\cot\theta_\psi^1, \cot\theta_\psi^2, \cot\theta_\psi^3) , \quad \cot\theta_\psi = c_\psi/s_\psi . \quad (25)$$

Comparing with Eq. (15), in this model we obtain $A = I$ and $B = \cot\psi$, a diagonal matrix.

Rotating the chiral fermions to the mass basis, the diagonal coefficients of the second term of Eq. (24) lead to:

$$g_{P\psi^i\psi^i} \frac{v}{\Lambda} = \frac{m_{\psi^i}}{f} \sum_j |U_{\psi_R}|_{ji}^2 \cot\theta_\psi^j \simeq \frac{m_{\psi^i}}{f} \cot\theta_\psi^i , \quad (26)$$

where in the right-hand-side we have made the assumption that the term with $j = i$ dominates, that will be the case when the mixing angles are small and the ratio $\cot\theta_\psi^j/\cot\theta_\psi^i$ does not compensate the smallness of those mixings.

Although $\cot\psi$ is diagonal, if its elements are not universal, it does not commute with U_{ψ_R} and generates flavor violating interactions $y_{P\psi^i\psi^j}$. For $i \neq j$:

$$(U_{\psi_R}^\dagger \cot\psi U_{\psi_R})_{ij} = (\cot\psi_2 - \cot\psi_1)(U_{\psi_R}^*)_{2i}(U_{\psi_R})_{2j} + (\cot\psi_3 - \cot\psi_1)(U_{\psi_R}^*)_{3i}(U_{\psi_R})_{3j} . \quad (27)$$

Since $\text{SO}(6)\sim\text{SU}(4)$, it contains anomalous representations. Fermions of the composite sector transforming with these representations contribute to the anomalous interactions with the fields of $\text{SO}(6)$:

$$c_s|_{\text{anom}} = 0 , \quad c_W|_{\text{anom}} = -c_B|_{\text{anom}} = n , \quad (28)$$

where n is an integer number. Unfortunately, in this model there are no anomalous contributions to the interactions with gluons, that could increase $\sigma(gg \rightarrow P)$ with small impact on σ_{4t} , neither with the photons, that could boost a signal in the clean $\gamma\gamma$ decay channel.

5.3.1 Matching

Making use of the previous results we can obtain the couplings of Eq. (1) in the $\text{SO}(6)/\text{SO}(5)$ model. From Eqs. (24) and (26) we get:

$$g_{\psi^i} \simeq \frac{m_{\psi^i}}{f} \cot\theta_\psi^i , \quad g_{gg} \simeq 4.2 \frac{g_s^2}{16\pi^2 f} \cot\theta_t . \quad (29)$$

Using the benchmark point with $x = 0$, described in Section 4, we get for the third generation:

$$\cot \theta_t \sim 4 \frac{f}{\text{TeV}}, \quad \cot \theta_b \sim 145 \frac{f}{\text{TeV}}, \quad \cot \theta_\tau \sim 23 \frac{f}{\text{TeV}}. \quad (30)$$

Notice that although $\cot \theta \sim 100$, it does not lead to large couplings with the pseudoscalar, since these couplings are proportional to the quark masses. In the case of flavor universal $\cot \theta$ one gets: $g_d \sim 2 \times 10^{-4}$, $g_s \sim 2.5 \times 10^{-3}$ and $g_b \sim 0.3$.

Thus by choosing these values for $\cot \theta$, the SO(6)/SO(5) model is able to reproduce the phenomenology described in the previous sections, in the case without anomalous interactions from the new sector.

5.3.2 Flavor transitions

Let us study now FCNC induced by P -exchange. The Wilson coefficient of Eq. (21) is given by

$$C_\psi^{ijkl} = \frac{1}{m_P^2} \frac{m_\psi^i}{f} \frac{m_\psi^k}{f} (U_{\psi_R}^\dagger \cot_\psi U_{\psi_R})_{ij} (U_{\psi_R}^\dagger \cot_\psi U_{\psi_R})_{kl}. \quad (31)$$

Using the estimates of Table 1 and Ref. [49] we can obtain bounds on

$$c_\psi^{(ij)} = \cot_\psi^i - \cot_\psi^j. \quad (32)$$

Taking $f = 1$ TeV and the Wilson coefficient as $C = (c/\text{TeV})^2$, we get the predictions and bounds of Table 2.

	Model prediction	Bounds	
	c	$\sqrt{\text{Re}(c^2)}$	$\sqrt{\text{Im}(c^2)}$
K^0	$2 \times 10^{-5} c_d^{(21)} + 3 \times 10^{-6} c_d^{(31)}$	1.4×10^{-4}	1×10^{-5}
D^0	$10^{-5} c_u^{(21)} + 5 \times 10^{-8} c_u^{(31)}$	4.4×10^{-4}	4.4×10^{-4}
B_d^0	$4 \times 10^{-4} (c_d^{(21)} + c_d^{(31)})$	8×10^{-4}	8×10^{-4}
B_s^0	$2 \times 10^{-3} (c_d^{(21)} + c_d^{(31)})$	8×10^{-3}	8×10^{-3}

Table 2: Wilson coefficients for meson mixing. Defining the Wilson coefficient as $C = (c/\text{TeV})^2$ and taking $f = 1$ TeV, the second column shows the estimates for c in the model, the third and fourth columns show the bounds on the real and imaginary parts of these coefficients [49].

From Table 2 and assuming real Wilson coefficients, we obtain that the values $c_d^{(21)} \sim 5$ and $c_d^{(31)} \sim 34$ saturate the bound from K -system, whereas B_d requires $c_d^{(21)} + c_d^{(31)} \lesssim 2$ and B_s : $c_d^{(21)} + c_d^{(31)} \lesssim 4$ for saturation. Since $\cot \theta_b \sim 100$, constraints from B -meson mixing require a cancellation in $c_d^{(ij)}$ of order few percent, with one more order of magnitude for complex coefficients with arbitrary phases.

Bounds from D mesons allow $c_u^{(21)} \sim 44$, while constraints on $c_u^{(31)}$ are very soft. Since $\cot \theta_t \sim 5$, no tuning is needed to satisfy these bounds.

For leptons, there are strong bounds from $\mu \rightarrow 3e$ and $\tau \rightarrow \ell \ell' \ell''$, with ℓ being muons and electrons. However, since the couplings involved are suppressed by the initial and final lepton

masses, for $\cot \theta_e^i \lesssim \mathcal{O}(30)$ the predicted flavor violating BRs are several orders of magnitude below the bounds.

Summarizing, departures from universality must be lower than few percent (permil) for the down sector in the case of real (complex) coefficients, demanding either tuning or flavor symmetries and departure from anarchy, whereas they can be of order one for the up sector and leptons.

5.4 A model with P from a broken $U(1)$

The coset $SO(5) \times U(1)_P \times U(1)_X / SO(4) \times U(1)_X$ also delivers the Higgs and the pseudoscalar as NGBs from a strongly interacting sector.⁷ The Higgs emerges from the same coset as in the well known minimal composite Higgs model, namely, $SO(5)/SO(4)$, whereas P emerges from the spontaneous breaking of $U(1)_P$. The extra $U(1)$ factor is not spontaneously broken and it is required to accommodate the hypercharge of the SM fermions, with $Y = T_R^3 + X$. Since the NGBs arise from different factors of the symmetry group, H and P can have different decay constants. We assume that the same dynamics is responsible for the spontaneous breaking of both factors and take them of the same order.

The NGB unitary matrices are given by:

$$U_H = \exp(i\sqrt{2}h^{\hat{a}}T^{\hat{a}}/f_H) ; \quad U_P = \exp(i\sqrt{2}PQ_P/f_P) ; \quad (33)$$

where $T^{\hat{a}}$ and Q_P are the broken generators of $SO(5)$ and $U(1)_P$. For a state with well defined charge Q_P , U_P is just a phase.

In order to determine the interactions of the NGBs with the SM fermions, one has to choose an embedding into representations of $SO(5) \times U(1)_P \times U(1)_X$. A simple and realistic case can be obtained by considering the following:

$$\mathcal{O}_{q,u} \sim \mathbf{5}_{2/3,p_{q,u}} , \quad \mathcal{O}_d \sim \mathbf{10}_{2/3,p_d} , \quad \mathcal{O}_l \sim \mathbf{5}_{0,p_l} , \quad \mathcal{O}_e \sim \mathbf{10}_{0,p_e} . \quad (34)$$

The first and second subscripts in Eq. (34) are the $U(1)_X$ and $U(1)_P$ charges, respectively. The values of Q_P are *a priori* arbitrary.

Again the linear interactions of partial compositeness explicitly break the global symmetry and generate a potential for the NGBs. Ref. [25] has shown that, to generate a potential for P , at least one SM fermion must interact with two operators of the new sector with different p -charges. Following that reference we introduce two embeddings for u_R , with different charges under $U(1)_P$: p_u^1 and p_u^2 .

At energies below the TeV, where the massive resonances can be integrated, ones obtains Yukawa interactions:

$$\begin{aligned} \mathcal{L}_{\text{eff}} \supset & \bar{u}_L u_R \left[\frac{h}{v} m_u + i\sqrt{2} \frac{P}{f_P} (p_q m_u - m_u p_u) \right] + \bar{d}_L d_R \left[\frac{h}{v} m_d + i\sqrt{2} \frac{P}{f_P} (p_q m_d - m_d p_d) \right] \\ & + \bar{e}_L e_R \left[\frac{h}{v} m_e + i\sqrt{2} \frac{P}{f_P} (p_l m_e - m_e p_e) \right] \end{aligned} \quad (35)$$

with $p_u = (p_{u1} + p_{u2})/2$. In the case of one generation only, to leading order the P couplings are proportional to the Higgs ones, being determined by the Q_P charges and f_P . In the case of three generations p_ψ are diagonal matrices, thus the alignment with the Higgs coupling depends on whether Q_P is universal for the three generations or not. Comparing with Eq. (15), in this model we obtain $A = \sqrt{2}p_{\psi_L}$ and $B = -\sqrt{2}p_{\psi_R}$.

⁷A conserved $SU(3)$ factor accounting for color is understood.

If the diagonal terms dominate the sums, the flavor conserving coupling can be approximated by:

$$g_{P\psi^i\psi^i} \frac{v}{\Lambda} = \sqrt{2} \frac{m_{\psi^i}}{f} \sum_j (|U_{\psi_L}|_{ji}^2 p_{\psi_L}^{(j)} - |U_{\psi_R}|_{ji}^2 p_{\psi_R}^{(j)}) \simeq \sqrt{2} \frac{m_{\psi^i}}{f} (p_{\psi_L}^{(i)} - p_{\psi_R}^{(i)}) . \quad (36)$$

The flavor violating couplings have now contributions from Left- and Right-handed unitary matrices, for $i \neq j$:

$$g_{P\psi^i\psi^j} \frac{v}{\Lambda} = [(p_{\psi_L}^2 - p_{\psi_L}^1)(U_{\psi_L}^*)_{2i}(U_{\psi_L})_{2j} + (p_{\psi_L}^3 - p_{\psi_L}^1)(U_{\psi_L}^*)_{3i}(U_{\psi_L})_{3j}] \frac{m_{\psi^j}}{f_P} - [(p_{\psi_R}^2 - p_{\psi_R}^1)(U_{\psi_R}^*)_{2i}(U_{\psi_R})_{2j} + (p_{\psi_R}^3 - p_{\psi_R}^1)(U_{\psi_R}^*)_{3i}(U_{\psi_R})_{3j}] \frac{m_{\psi^i}}{f_P} . \quad (37)$$

The triangle anomaly with one $U(1)_P$ and two $SU(3)_c$ or $SO(5)$ generators gives anomalous couplings [29], for a multiplet of composite fermions f :

$$c_s|_{\text{anom}} = \sum_f p_f d_2^{(f)} I_3^{(f)} , \quad c_W|_{\text{anom}} = \sum_f p_f d_3^{(f)} I_2^{(f)} , \quad c_B|_{\text{anom}} = \sum_f p_f d_2^{(f)} d_3^{(f)} (Y^{(f)})^2 , \quad (38)$$

where d_2 and d_3 (I_2 and I_3) are the dimensions (indices) of the representations under $SU(2)_L$ and $SU(3)_c$, respectively. In the present example, for each generation of fermionic resonances transforming as in Eq. (34), taking $p_f = 1$ for all the fermions, one obtains: $c_s \simeq 12$, $c_W \simeq 22$ and $c_B \simeq 14$.

5.4.1 Matching

To reproduce the phenomenology, we match the couplings of Eq. (1) in the $SO(5) \times U(1)/SO(4)$ model. From Eqs. (35) and (36) we obtain:

$$g_t \simeq \sqrt{2} \frac{m_t}{f_P} (p_q^{(3)} - p_u^{(3)}) , \quad g_b \simeq \sqrt{2} \frac{m_b}{f_P} (p_q^{(3)} - p_d^{(3)}) , \quad g_\tau \simeq \sqrt{2} \frac{m_\tau}{f_P} (p_l^{(3)} - p_e^{(3)}) . \quad (39)$$

Taking into account Eq. (13), we obtain for the anomalous coupling to gluons,

$$g_{gg} \simeq \frac{g_s^2}{16\pi^2 f_P} \left[4.2\sqrt{2}(p_q^{(3)} - p_u^{(3)}) + 4c_s|_{\text{anom}} \right] , \quad (40)$$

with $c_s|_{\text{anom}}$ given in Eq. (38). Similar expressions can be derived for EW gauge bosons.

For the benchmark points we get:

$$p_q^{(3)} - p_u^{(3)} \simeq 2.6 \frac{f_P}{\text{TeV}} , \quad p_q^{(3)} - p_d^{(3)} \sim 10^2 \frac{f_P}{\text{TeV}} , \quad p_l^{(3)} - p_e^{(3)} \sim 20 \frac{f_P}{\text{TeV}} . \quad (41)$$

The bottom-quark requires charges $\mathcal{O}(100)$. The global current associated to the symmetry $U(1)_P$ is expected to create spin one composite states, that can couple to the composite fermions with coupling \tilde{g}_* and charge Q_P . A well defined perturbative description of the theory of resonances requires $\tilde{g}_* Q_P \ll 4\pi$, thus for charges $\mathcal{O}(100)$ one has to demand $\tilde{g}_* \ll 0.1$. However, since the mass of the spin-one state is estimated as $\sim g_* f_P$, for such a small $U(1)_P$ coupling one would expect a very light resonance. This is in fact expected given that for such a large charge the UV-running would imply a Landau pole at low energies, signaled by the presence of low mass resonances. We consider this to be a more serious problem than the flavor constraints discussed in the next section, that depend on several assumptions in the UV. Therefore, this model is in strong tension with the

large coupling g_b , that is required at 68% CL by the τ -channel with pseudoscalar production by bottom fusion. However this strong tension can be alleviated by considering the 95% CL limits, that contain a region with $g_b = 0$ and $g_\tau \gtrsim 0.023$, requiring $(p_l^{(3)} - p_e^{(3)}) \sim 10$.

For the second benchmark point, where an anomalous contribution to the gluon coupling is included, taking $x \sim 0.13 \pm 0.05$ we obtain:

$$\sum_f p_f d_2^{(f)} \simeq (1.4 - 2.7) \frac{f_P}{\text{TeV}}. \quad (42)$$

5.4.2 Flavor

Using the couplings of Eq. (37) in (21) one obtains the Wilson coefficients induced by P -exchange in this model. The bounds on deviations from universality of $p_{\psi_R}^{(i)}$ are as in Table 2, changing $c_\psi^{(ij)}$ by $\Delta p_{\psi_R}^{(ij)} \equiv (p_{\psi_R}^{(j)} - p_{\psi_R}^{(i)})$. Thus the constraints on $c_\psi^{(ij)}$ apply also to $\Delta p_{\psi_R}^{(ij)}$. For leptons, in the Left-Right symmetric limit, constraints on $\Delta p_l^{(ij)}$ are similar to those on $\Delta p_e^{(ij)}$.

In this model there are as well bounds on $\Delta p_{\psi_L}^{(ij)}$, that can be obtained by a similar calculation, taking into account that the Left-handed angles are of CKM size. Assuming real Wilson coefficients, for the Kaon system we get: $\Delta p_q^{(21)} \lesssim 7$ and $\Delta p_q^{(31)} \lesssim 3 \times 10^3$, for B_d : $\Delta p_q^{(21)}, \Delta p_q^{(31)} \lesssim 17$ and for B_s : $\Delta p_q^{(21)}, \Delta p_q^{(31)} \lesssim 34$. Since the estimate of Eq. (41) gives $(p_q^{(3)} - p_d^{(3)}) \gtrsim 10^2$, the constraints from meson mixing require cancellations at few percent level, whereas for complex coefficients the tuning is at permil level. For D mesons $\Delta p_q^{(21)} \lesssim 2$, while constraints on $\Delta p_q^{(31)}$ are very soft.

6 Conclusions

Several experimental results from the LHC could be pointing to a new pseudoscalar state at 400 GeV, mostly coupled to the third generation of fermions. Results from CMS in the $t\bar{t}$ final state as well as the results from ATLAS in the $\tau^+\tau^-$ channel, favor a pseudoscalar neutral particle that is produced via gluon fusion or in association with bottom-quarks. We have analyzed from a phenomenological perspective, initially in a bottom-up approach, the couplings that such state should have with those fermions and gauge bosons to be able to reproduce the different excesses, while at the same time keeping below the bounds the related channels that show no deviations with respect to the SM. Scanning over the parameter space of the most general CP-invariant interaction Lagrangian linear in the pseudoscalar state a that can be written up to dimension-5 operators, we have found regions in which the new physics hints, as well as all experimental constraints, can be satisfied and in which the pseudoscalar coupling to gluons can be induced by the SM top quark, that gives by far the dominant contribution, but there can also be room for contributions from heavy new states. We found that the couplings of the pseudoscalar to top quarks and τ leptons are of the same order of magnitude as the Higgs ones, while the coupling to bottom-quarks is required to be $\sim 20 - 30$ times larger than the one for the Higgs.

Though our low-energy phenomenological effective model satisfies all current experimental bounds and provides an explanation for the hints in ditop and ditau final states for the regions of parameter space considered, one may wonder in which of these and/or other channels one could expect to find a signal for the presence of the pseudoscalar in future measurements. In this aspect, one of the channels in which one would expect to be able to probe the previous scenario in the future is in the production of 4-tops in which there is a currently an excess that is around twice the SM one. Furthermore, given the hint of an excess in the $\tau^+\tau^-$ channel initiated by b -quarks,

one could also expect the pseudoscalar to provide an excess in the $b\bar{b}$ final states in future measurements. On the other hand diboson channels are more model dependent due to their possible UV contributions, thus there are no robust predictions for diboson final states, though one would expect any possible signal to show first in the diphoton channel due to its cleanness.

We have also considered a set of gauge invariant models, analyzing their capability to reproduce the collider phenomenology related with the hints at 400 GeV. We have found that, although usual 2HDMs of Type I-IV cannot reproduce the pseudoscalar couplings required by the phenomenology, more sophisticated models as SFV 2HDM could in principle do it [16]. However the contributions of this model to flavor changing processes, induced at radiative level by exchange of a charged Higgs, require the masses of these states to be above ~ 3 TeV, demanding quartic couplings above the perturbative regime to split the pseudo scalar mass m_A from the CP-even heavy Higgs mass m_H . On a different direction, models with a new strongly interacting sector leading to a light pseudoscalar singlet could also potentially reproduce the LHC phenomenology we wish to address. We have analyzed two specific realizations that have already been considered in the literature, although in a different context. One of the models contains a composite state that is a pseudo Nambu Goldstone boson arising from an spontaneous breaking of $SO(6)/SO(5)$, which Yukawa couplings are aligned with the Higgs ones. In this model $SO(6)$ anomalies can generate contributions to the couplings with EW massive gauge bosons, but not with the gluons or photons. Under the assumption of flavor anarchy, bounds from mixing in Kaon and B -meson systems require tuning to obtain an approximate universal factor in the down sector, another interesting possibility that requires a dedicated analysis would be the introduction of flavor symmetries. The other model we consider is based on the coset $SO(5) \times U(1)_P \times U(1)_X / SO(4) \times U(1)_X$, in which the light state arises from an spontaneous breaking of a $U(1)_P$ symmetry of the new sector, that can also generate anomalous contributions to the couplings with gluons and photons. However at 1σ level the coupling of the bottom-quark demands $U(1)$ charges of new composite fermions $\sim \mathcal{O}(100)$, introducing some tension. At 2σ level this requirement is relaxed, since the $\tau^+\tau^-$ channel with initial b -quarks is compatible with the SM.

Last, it would be interesting to study models with a pseudoscalar arising from other cosets, in particular with unified groups, where one could expect to obtain contributions to the gluon coupling from the anomaly, as well as models with elementary weakly-coupled states.

Acknowledgments

The authors would like to thank Ezequiel Álvarez for help with MGME and Víctor Martín-Lozano for collaboration in the beginning of this article and for fruitful discussions. The work of EA is partially supported by the “Atracción de Talento” program (Modalidad 1) of the Comunidad de Madrid (Spain) under the grant number 2019-T1/TIC-14019 and by the Spanish Research Agency (Agencia Estatal de Investigación) through the grant IFT Centro de Excelencia Severo Ochoa SEV-2016-0597. The work is also partially supported by CONICET and ANPCyT under projects PICT 2016-0164, PICT 2017-2751, PICT 2017-0802, PICT 2017-2765 and PICT 2018-03682.

References

- [1] ATLAS collaboration, *Observation of a new particle in the search for the Standard Model Higgs boson with the ATLAS detector at the LHC*, *Phys. Lett. B* **716** (2012) 1 [1207.7214].
- [2] CMS collaboration, *Observation of a New Boson at a Mass of 125 GeV with the CMS Experiment at the LHC*, *Phys. Lett. B* **716** (2012) 30 [1207.7235].

- [3] CMS collaboration, *Search for heavy Higgs bosons decaying to a top quark pair in proton-proton collisions at $\sqrt{s} = 13$ TeV*, *JHEP* **04** (2020) 171 [[1908.01115](#)].
- [4] ATLAS collaboration, *Search for heavy Higgs bosons decaying into two tau leptons with the ATLAS detector using pp collisions at $\sqrt{s} = 13$ TeV*, *Phys. Rev. Lett.* **125** (2020) 051801 [[2002.12223](#)].
- [5] ATLAS collaboration, *Search for Scalar Diphoton Resonances in the Mass Range 65 – 600 GeV with the ATLAS Detector in pp Collision Data at $\sqrt{s} = 8$ TeV*, *Phys. Rev. Lett.* **113** (2014) 171801 [[1407.6583](#)].
- [6] CMS collaboration, *Search for diphoton resonances in the mass range from 150 to 850 GeV in pp collisions at $\sqrt{s} = 8$ TeV*, *Phys. Lett. B* **750** (2015) 494 [[1506.02301](#)].
- [7] ATLAS collaboration, *Search for new phenomena in high-mass diphoton final states using 37 fb^{-1} of proton-proton collisions collected at $\sqrt{s} = 13$ TeV with the ATLAS detector*, *Phys. Lett. B* **775** (2017) 105 [[1707.04147](#)].
- [8] ATLAS collaboration, *Searches for the $Z\gamma$ decay mode of the Higgs boson and for new high-mass resonances in pp collisions at $\sqrt{s} = 13$ TeV with the ATLAS detector*, *JHEP* **10** (2017) 112 [[1708.00212](#)].
- [9] ATLAS collaboration, *Search for heavy resonances decaying into a W or Z boson and a Higgs boson in final states with leptons and b-jets in 36 fb^{-1} of $\sqrt{s} = 13$ TeV pp collisions with the ATLAS detector*, *JHEP* **03** (2018) 174 [[1712.06518](#)].
- [10] CMS collaboration, *Search for beyond the standard model Higgs bosons decaying into a $b\bar{b}$ pair in pp collisions at $\sqrt{s} = 13$ TeV*, *JHEP* **08** (2018) 113 [[1805.12191](#)].
- [11] CMS collaboration, *Search for a heavy pseudoscalar boson decaying to a Z and a Higgs boson at $\sqrt{s} = 13$ TeV*, *Eur. Phys. J. C* **79** (2019) 564 [[1903.00941](#)].
- [12] CMS collaboration, *Search for a heavy pseudoscalar Higgs boson decaying into a 125 GeV Higgs boson and a Z boson in final states with two tau and two light leptons at $\sqrt{s} = 13$ TeV*, *JHEP* **03** (2020) 065 [[1910.11634](#)].
- [13] CMS collaboration, *Search for new neutral Higgs bosons through the $H \rightarrow ZA \rightarrow \ell^+ \ell^- b\bar{b}$ process in pp collisions at $\sqrt{s} = 13$ TeV*, *JHEP* **03** (2020) 055 [[1911.03781](#)].
- [14] ATLAS collaboration, *Evidence for $t\bar{t}t$ production in the multilepton final state in proton-proton collisions at $\sqrt{s} = 13$ TeV with the ATLAS detector*, *Eur. Phys. J. C* **80** (2020) 1085 [[2007.14858](#)].
- [15] F. Richard, *Evidences for a pseudo scalar resonance at 400 GeV Possible interpretations*, [2003.07112](#).
- [16] D. Egana-Ugrinovic, S. Homiller and P. R. Meade, *Higgs bosons with large couplings to light quarks*, *Phys. Rev. D* **100** (2019) 115041 [[1908.11376](#)].
- [17] D. B. Kaplan and H. Georgi, *$SU(2) \times U(1)$ Breaking by Vacuum Misalignment*, *Phys. Lett. B* **136** (1984) 183.
- [18] D. B. Kaplan, H. Georgi and S. Dimopoulos, *Composite Higgs Scalars*, *Phys. Lett. B* **136** (1984) 187.
- [19] H. Georgi, D. B. Kaplan and P. Galison, *Calculation of the Composite Higgs Mass*, *Phys. Lett. B* **143** (1984) 152.
- [20] H. Georgi and D. B. Kaplan, *Composite Higgs and Custodial $SU(2)$* , *Phys. Lett. B* **145** (1984) 216.
- [21] M. J. Dugan, H. Georgi and D. B. Kaplan, *Anatomy of a Composite Higgs Model*, *Nucl. Phys. B* **254** (1985) 299.
- [22] R. Contino, Y. Nomura and A. Pomarol, *Higgs as a holographic pseudoGoldstone boson*, *Nucl. Phys. B* **671** (2003) 148 [[hep-ph/0306259](#)].

- [23] K. Agashe, R. Contino and A. Pomarol, *The Minimal composite Higgs model*, *Nucl. Phys. B* **719** (2005) 165 [[hep-ph/0412089](#)].
- [24] B. Gripaios, A. Pomarol, F. Riva and J. Serra, *Beyond the Minimal Composite Higgs Model*, *JHEP* **04** (2009) 070 [[0902.1483](#)].
- [25] M. Chala, G. Durieux, C. Grojean, L. de Lima and O. Matsedonskyi, *Minimally extended SILH*, *JHEP* **06** (2017) 088 [[1703.10624](#)].
- [26] ATLAS collaboration, *Search for heavy resonances decaying into WW in the $e\nu\mu\nu$ final state in pp collisions at $\sqrt{s} = 13$ TeV with the ATLAS detector*, *Eur. Phys. J. C* **78** (2018) 24 [[1710.01123](#)].
- [27] ATLAS collaboration, *Search for heavy resonances decaying into a pair of Z bosons in the $\ell^+\ell^-\ell'^+\ell'^-$ and $\ell^+\ell^-\nu\bar{\nu}$ final states using 139 fb^{-1} of proton–proton collisions at $\sqrt{s} = 13$ TeV with the ATLAS detector*, *Eur. Phys. J. C* **81** (2021) 332 [[2009.14791](#)].
- [28] CMS collaboration, *Search for a new scalar resonance decaying to a pair of Z bosons in proton-proton collisions at $\sqrt{s} = 13$ TeV*, *JHEP* **06** (2018) 127 [[1804.01939](#)].
- [29] R. Franceschini, G. F. Giudice, J. F. Kamenik, M. McCullough, A. Pomarol, R. Rattazzi et al., *What is the $\gamma\gamma$ resonance at 750 GeV?*, *JHEP* **03** (2016) 144 [[1512.04933](#)].
- [30] J. Alwall, R. Frederix, S. Frixione, V. Hirschi, F. Maltoni, O. Mattelaer et al., *The automated computation of tree-level and next-to-leading order differential cross sections, and their matching to parton shower simulations*, *JHEP* **07** (2014) 079 [[1405.0301](#)].
- [31] CMS collaboration, *Search for heavy Higgs bosons decaying to a top quark pair in proton-proton collisions at $\sqrt{s} = 13$ TeV*, *JHEP* **04** (2020) 171 [[1908.01115](#)].
- [32] M. Bonvini, A. S. Papanastasiou and F. J. Tackmann, *Matched predictions for the $b\bar{b}H$ cross section at the 13 TeV LHC*, *JHEP* **10** (2016) 053 [[1605.01733](#)].
- [33] ATLAS collaboration, *Evidence for $t\bar{t}t\bar{t}$ production in the multilepton final state in proton–proton collisions at $\sqrt{s} = 13$ TeV with the ATLAS detector*, *Eur. Phys. J. C* **80** (2020) 1085 [[2007.14858](#)].
- [34] B. Gripaios and S. M. West, *Anomaly holography*, *Nucl. Phys. B* **789** (2008) 362 [[0704.3981](#)].
- [35] B. Gripaios, *Anomaly Holography, the Wess-Zumino-Witten Term, and Electroweak Symmetry Breaking*, *Phys. Lett. B* **663** (2008) 419 [[0803.0497](#)].
- [36] K. Agashe and R. Contino, *The Minimal composite Higgs model and electroweak precision tests*, *Nucl. Phys. B* **742** (2006) 59 [[hep-ph/0510164](#)].
- [37] B. Gripaios, M. Nardecchia and T. You, *On the Structure of Anomalous Composite Higgs Models*, *Eur. Phys. J. C* **77** (2017) 28 [[1605.09647](#)].
- [38] R. Contino and A. Pomarol, *Holography for fermions*, *JHEP* **11** (2004) 058 [[hep-th/0406257](#)].
- [39] B. Bellazzini, R. Franceschini, F. Sala and J. Serra, *Goldstones in Diphotons*, *JHEP* **04** (2016) 072 [[1512.05330](#)].
- [40] J. Wess and B. Zumino, *Consequences of anomalous Ward identities*, *Phys. Lett. B* **37** (1971) 95.
- [41] E. Witten, *Global Aspects of Current Algebra*, *Nucl. Phys. B* **223** (1983) 422.
- [42] J. Davighi and B. Gripaios, *Topological terms in Composite Higgs Models*, *JHEP* **11** (2018) 169 [[1808.04154](#)].
- [43] K. Agashe, G. Perez and A. Soni, *Flavor structure of warped extra dimension models*, *Phys. Rev. D* **71** (2005) 016002 [[hep-ph/0408134](#)].
- [44] C. Csaki, A. Falkowski and A. Weiler, *The Flavor of the Composite Pseudo-Goldstone Higgs*, *JHEP* **09** (2008) 008 [[0804.1954](#)].
- [45] G. Panico and A. Wulzer, *The Composite Nambu-Goldstone Higgs*, vol. 913. Springer, 2016, [10.1007/978-3-319-22617-0](#), [[1506.01961](#)].

- [46] J. A. Aguilar-Saavedra, *A Minimal set of top-Higgs anomalous couplings*, *Nucl. Phys. B* **821** (2009) 215 [[0904.2387](#)].
- [47] K. Agashe and R. Contino, *Composite Higgs-Mediated FCNC*, *Phys. Rev. D* **80** (2009) 075016 [[0906.1542](#)].
- [48] K. Agashe, R. Contino, L. Da Rold and A. Pomarol, *A Custodial symmetry for $Zb\bar{b}$* , *Phys. Lett. B* **641** (2006) 62 [[hep-ph/0605341](#)].
- [49] UTFIT collaboration, *Model-independent constraints on $\Delta F = 2$ operators and the scale of new physics*, *JHEP* **03** (2008) 049 [[0707.0636](#)].